Electronic Supplementary Material (ESI) for Sustainable Energy & Fuels.

Mono-Transition-Metal-substituted Polyoxometalates as Shuttle Redox Mediator for Z-scheme Water Splitting under Visible Light

Osamu Tomita, [a] *Hiroki Naito,* [a] *Akinobu Nakada,* [a] *Masanobu Higashi* [a] *and Ryu Abe*[*a b]

[a] Graduate School of Engineering, Kyoto University, Katsura, Nishikyo-ku, Kyoto 615-8510, Japan.

[b] CREST, Japan Science and Technology Agency (JST), Kawaguchi, Saitama, 332-0012, Japan.

E-mail: ryu-abe@scl.kyoto-u.ac.jp; Fax: +81 75 383 2479; Tel: +81 75 383 2479

1. Reagents for preparation of polyoxometalates and photocatalyst particles

All the commercial reagents and solvents shown below were used as received. Sodium tungstate dihydrate ($Na_2WO_4 \cdot 2H_2O$, 99.0%, Wako Pure Chemical Corporation), sodium metasilicate nonahydrate ($Na_2SiO_3 \cdot 9H_2O$, 98.0%, Wako Pure Chemical Corporation), boric acid (H_3BO_3, 99.5 %, Wako Pure Chemical Corporation), sodium metavanadate ($NaVO_3$, 90%, Wako Pure Chemical Corporation), vanadium oxide sulfate *n*-hydrate ($VOSO_4 \cdot nH_2O$, 99.9%, Wako Pure Chemical Corporation), tungstosilicic acid *n*-hydrate ($H_4[SiW_{12}O_{40}] \cdot nH_2O$, 99.9%, Sigma-Aldrich), 12 tungsto(VI) phosphoric acid *n*-hydrate ($H_3PW_{12}O_{40} \cdot nH_2O$, Wako Pure Chemical

Corporation), cobalt(II) acetate tetrahydrate ($Co(CH_3COO)_2 \cdot 4H_2O$, 99.0%, Wako Pure Chemical Corporation), manganese(II) sulfate pentahydrate ($MnSO_4 \cdot 5H_2O$, 99.9%, Wako Pure Chemical Corporation), potassium chloride (KCl, 99.5%, Wako Pure Chemical Corporation), hydrochloric acid (HCl, 35~37%, Wako Pure Chemical Corporation), acetic acid (CH_3COOH, 99.7%, Wako Pure Chemical Corporation), potassium acetate (CH_3COOK, 97.0%, Wako Pure Chemical Corporation), potassium hydrogen carbonate ($KHCO_3$, 99.5%, Wako Pure Chemical Corporation), lithium carbonate (Li_2CO_3, 99.0%, Wako Pure Chemical Corporation), potassium dihydrogen phosphate (KH_2PO_4, 99.5%, Wako Pure Chemical Corporation), potassium hydroxide (KOH, 90%, Kishida Chemical Co., Ltd.), potassium bromide (KBr, 99.0%, Wako Pure Chemical Corporation), tungsten oxide (WO_3, 99.99%, Kojundo Chemical Laboratory Co., Ltd., mixture of triclinic and monoclinic, 4.8 $m^2\ g^{-1}$), hydrogen hexachloroplatinate(IV) hexahydrate ($H_2PtCl_6 \cdot 6H_2O$, 99.9%, Wako Pure Chemical Corporation), strontium carbonate ($SrCO_3$, 99.99%, Wako Pure Chemical Corporation), titanium(IV) oxide (TiO_2, rutile, 99.0%, Wako Pure Chemical Corporation), rhodium(III) oxide (Rh_2O_3, 98~102 %, Wako Pure Chemical Corporation), ruthenium(III) chloride *n*-hydrate ($RuCl_3 \cdot nH_2O$, 99.9%, Wako Pure Chemical Corporation).

2. Preparation of polyoxometalate

2. 1. Preparation of $K_6[SiW_{11}O_{39}Co^{II}(H_2O)] \cdot nH_2O$

A Co-substituted Keggin-type silicotungstate *n*-hydrate ($K_6[SiW_{11}O_{39}Co^{II}(H_2O)] \cdot nH_2O$) was prepared from the $H_4[SiW_{12}O_{40}] \cdot nH_2O$ as follows according to a previously reported method.[1] 2 mmol of $H_4[SiW_{12}O_{40}] \cdot nH_2O$ was dissolved into an CH_3COOH aq. solution (12 vol%, 13 mL)

and the pH was adjusted to 6.0 with $KHCO_3$. The solution was heated around 70 °C with stirring by magnetic stirrer, and 1.6 mmol of $Co(CH_3COO)_2 \cdot 4H_2O$ in 4 mL of hot Milli-Q water (70 °C) was added, followed by 7.5 g of CH_3COOK in CH_3COOH aq. solution (6 vol%, 4 mL) and then kept for 4 min. Resulting hot solution was filtered and kept at 5 °C for 15 h. Precipitates with deep red crystal form were recrystallized twice from hot Milli-Q water (2 mL each). The obtained samples will be denoted as $SiCo^{II}$ hereafter. The hydration number determined by using TG was 11. Anal. Calc. for $K_6[SiW_{11}O_{39}Co^{II}(H_2O)] \cdot 11H_2O$, K: 7.4, Si: 0.9, Co: 1.9, W: 63.5 wt.%. Found, K: 6.4, Si: 0.8, Co: 1.6, W: 63.5 wt.%.; H_2O: 7.3 wt.%

2. 2. Preparation of $K_4[\alpha\text{-}PV^VW_{11}O_{40}] \cdot nH_2O$

A V-substituted Keggin-type phosphotungstate *n*-hydrate ($K_4[PV^VW_{11}O_{40}] \cdot nH_2O$) was prepared from the $H_3PW_{12}O_{40} \cdot nH_2O$ as follows according to a previously reported method.[2] 9.4 mmol of $H_3PW_{12}O_{40} \cdot nH_2O$ was dissolved into 25 mL of Milli-Q water, and pH of the solution was adjusted to 4.9 by the addition of Li_2CO_3. Then, the solution was diluted to 37.5 mL total by Milli-Q water and $NaVO_3$ aq. (0.2 M, 50 mL) was add to the solution under continuous stirring by magnetic stirrer. After pH of the solution was adjusted to 2.0 by addition of HCl aq. (6 M), the solution was heated to 60 °C and kept for 10 min. After the solution was cooled to room temperature (pH 3.3), pH was readjusted to 2.0 by HCl (6 M). The solution was reheated to 60 °C and 10 g of KCl was added and solution was maintained at 60 °C for further 10 min. After cooling to room temperature, solution was filtered. The obtained filtrate was washed with 10 mL of Milli-Q water twice, affording a canary yellow powder, $K_4[PV^VW_{11}O_{40}] \cdot nH_2O$ (denoted as PV^V hereafter). The hydration number determined by using TG was 4. Anal. Calc. for

$K_4[PV^VW_{11}O_{40}]\cdot 4H_2O$, K: 5.3, P: 1.0, V: 1.7, W: 68.0 wt.%. Found, K: 5.1, P: 1.1, V: 1.7, W: 66.0 wt.%.; H_2O: 2.7 wt.%

2. 3. Preparation of $K_7[\alpha\text{-}BV^{IV}W_{11}O_{40}]\cdot nH_2O$

A V-substituted Keggin-type tungstoborate *n*-hydrate ($K_7[\alpha\text{-}BV^{IV}W_{11}O_{40}]\cdot nH_2O$) was prepared as follows according to a previously reported method.[3] 110 mmol of $Na_2WO_4\cdot 2H_2O$ was dissolved into 100 mL of Milli-Q water and pH of solution was adjusted to 6.3 with CH_3COOH. After 40 mmol of H_3BO_3 was dissolved to the solution, the temperature of the solution was increased to 80 °C under continuous stirring. And then 10 mmol of $VOSO_4\cdot nH_2O$ was added to the solution, and sequentially allowed to cool to room temperature under continuous stirring over one night. After 20 g of KCl was added to the solution, the precipitates were collected by filtration, recrystallized from acetate buffer (0.2 M of CH_3COOH/CH_3COOK, pH 5.1, 60 mL), and finally washed with 10 mL of Milli-Q water twice. During recrystallization process, insoluble species were once removed by filtration. The obtained samples will be denoted as BV^{IV} hereafter. The hydration number determined by using TG was 7. Anal. Calc. for $K_7[BV^{IV}W_{11}O_{40}]\cdot 7H_2O$, K: 8.8, B: 0.35, V: 1.6, W: 64.7 wt.%. Found, K: 7.8, B: 0.30, V: 1.4, W: 58.3 wt.%.; H_2O: 4.4 wt.%

2. 4. Preparation of Photocatalyst Particles

Commercially available WO_3 powder (mixture of triclinic and monoclinic phase, 4.8 $m^2\ g^{-1}$, Kojundo Chemical Laboratory Co., Ltd.) was used as photocatalysts. The aggregated large particles of WO_3, which have higher activity for O_2 evolution than fine particles (data not

shown), were collected from the commercial WO_3 samples as follows.[4,5] The as-purchased WO_3 powder (6.5 g), containing both fine particles and large aggregates, was suspended in Milli-Q water (approximately 50 mL) and exposed to ultrasonic dispersion for more than 10 min. The resultant suspension was then centrifuged at 1000 rpm for 10 min. After the supernatant containing fine WO_3 particle was collected in another bottle, an appropriate amount of Milli-Q water (approximately 50 mL) was added to the remaining suspension, still containing the mixture of fine and large particles. This suspension was again subjected to ultrasonic dispersion and subsequent centrifugation. After five repetitions of this process, the precipitated particles were collected and subsequent drying in air at 60 °C. The particles obtained were confirmed to consist of the monoclinic phase predominantly and have approximately 3.4 $m^2\ g^{-1}$ of specific surface area. The obtained large aggregated WO_3 powder was used.

Particles of strontium titanate doped with Rh species ($SrTiO_3$:Rh, Sr : Ti: Rh = 1.07 : 0.99: 0.01) was prepared by a solid-state reaction, according to previous reports.[6] Required amount of $SrCO_3$, TiO_2 and Rh_2O_3 were mixed well in agate mortar. Then the mixture was calcined at 800 °C for 2 h once and 1000 °C for 5 h twice in air, and the heating rate was fixed at 10 °C min^{-1} for all calcination temperatures. Samples were roughly mixed between each calcination. The obtained samples will be denoted as $SrTiO_3$:Rh hereafter. Ru species were loaded onto the $SrTiO_3$:Rh samples *via* the following photodeposition method. 1 g of $SrTiO_3$:Rh were suspended in an aqueous methanol solution (200 mL, 20 vol%) containing the required amount of $RuCl_3 \bullet nH_2O$ as precursor (0.7 wt.% as Ru metal). $SrTiO_3$:Rh samples were irradiated with visible light from a Xe lamp (LX-300F, Cermax 300 W, $\lambda > 400$ nm) as the light source for 5 h under Ar atmosphere. After 5 times repeated washings with Milli-Q water and centrifugation, the sample was dried in air, and employed as the H_2-evolving photocatalyst.

Figs. S1 and S2 shows the cyclic voltammograms of each POM. In all cases, the voltammograms were not changed with continuous cycles, therefore fifth cycles are shown as a representative. As shown in Fig. S1, the reversible peaks are observed for SiW_{11} in KH_2PO_4 electrolyte solution at –0.5 V, –0.9 V (vs. Ag/AgCl) which are corresponding to the reduction of W species in the framework, as previously reported.[7] As for transition metal-substituted POMs (Fig. S2), reversible peaks are observed for each sample at anodic potentials, which can be assigned to the redox cycles of SiV^{V}/ SiV^{IV} (half-wave potential ($E_{1/2}$) : +0.41 V vs. Ag/AgCl), $SiCo^{III}/SiCo^{II}$ ($E_{1/2}$: +1.05 V vs. Ag/AgCl), PV^{V}/PV^{IV} ($E_{1/2}$: + 0.62 V vs. Ag/AgCl), and BV^{V}/BV^{IV} ($E_{1/2}$: + 0.17 V vs. Ag/AgCl) species incorporated in the framework as well as the that of W species, as previously reported.[3,8–10]

1. T. J. R. Weakley and S. A. Malik, *J. Inorg. Nucl. Chem.*, 1967, **29**, 2935–2944.
2. P. J. Domaille, *J. Am. Chem. Soc.*, 1984, **106**, 7677–7687.
3. J. J. Altenau, M. T. Pope, R. A. Prados and H. So, *Inorg. Chem.*, 1975, **14**, 417–421.
4. R. Abe, H. Takami, N. Murakami, B. Ohtani, *J. Am. Chem. Soc.*, 2008, **130**, 7780–7781.
5. Tomita, T. Otsubo, M. Higashi, B. Ohtani, R. Abe, *ACS Catal.*, 2016, **6**, 1134–1144.
6. H. Kato, Y. Sasaki, N. Shirakura, A. Kudo, *J. Mater. Chem. A*, 2013, **1**, 12327–12333
7. K. Tsuji, O. Tomita, M. Higashi and R. Abe, *ChemSusChem*, 2016, **9**, 2201–2208.
8. C. Li, Y. Zhang, K. P. O'Halloran, J. Zhang and H. Ma, *J. Appl. Electrochem.*, 2009, **39**, 421–427.
9. J. L. Samonte and M. T. Pope, *Can. J. Chem.*, 2001, **79**, 802–808.
10. D. P. Smith and M. T. Pope, *Inorg. Chem.*, 1973, **12**, 331–336.

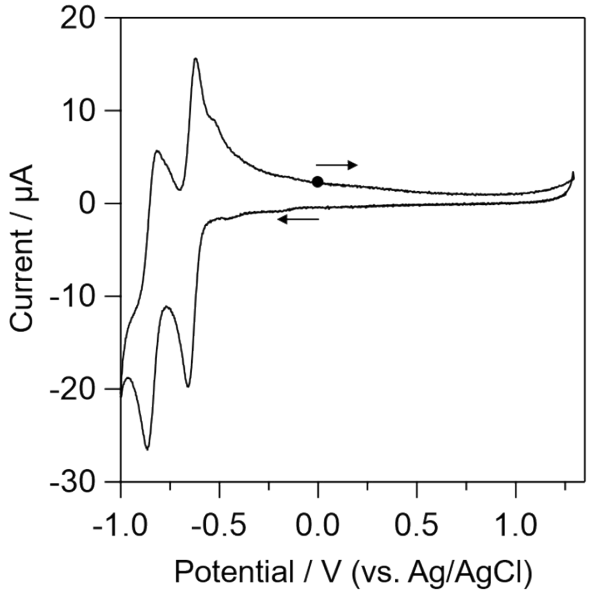

Fig. S1 Cyclic voltammogram of SiW_{11} (1 mM) in an aq. KH_2PO_4 solution (0.5 M, pH 4.4) (after fifth cycles; working electrode: GC, counter electrode: Pt coil; scan rate: 50 mV s^{-1}).

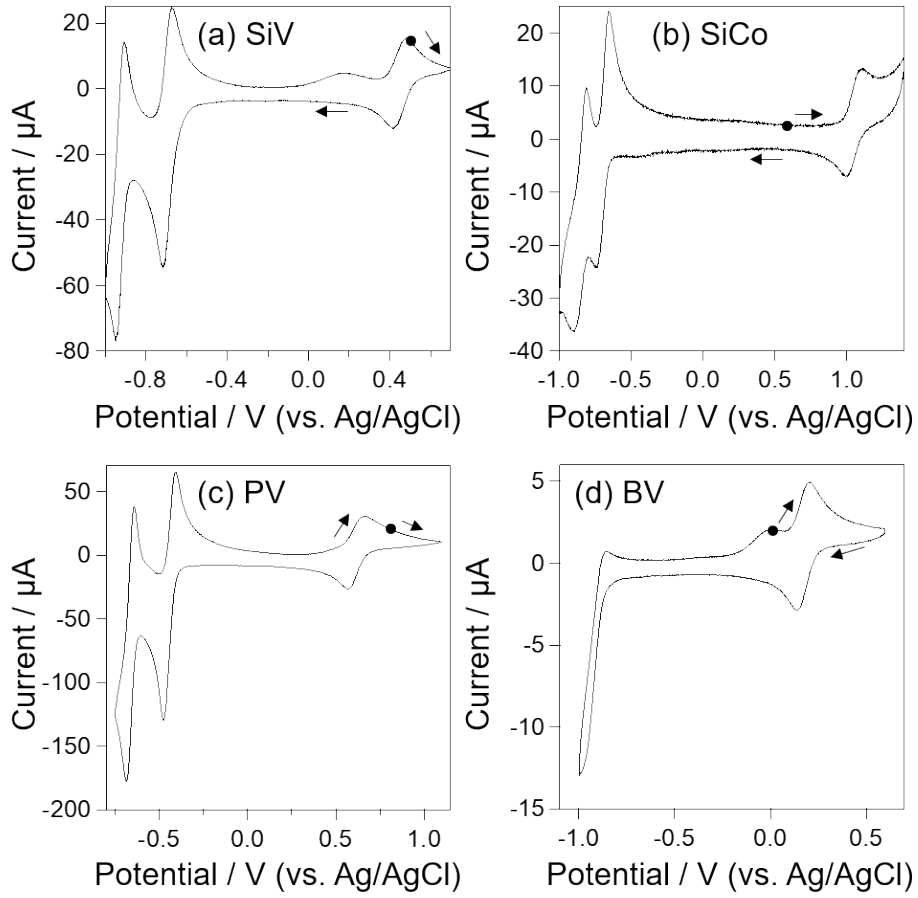

Fig. S2 Cyclic voltammograms of (a) SiV (2 mM) : AcOH/AcONa buffer (0.5 M, pH 4.5), (b) SiCo (1 mM) : AcOH/AcONa (0.1 M) + $NaClO_4$ (0.9 M) buffer (pH 4.7), (c) PV (2 mM) : AcOH/AcONa buffer (0.5 M, pH 4.5), and (d) BV (0.5 mM) : $Na_xH_{3-x}PO_4$ buffer (0.1 M, pH 6.0) (after fifth cycles; working electrode: GC, counter electrode: Pt coil; scan rate: 50 mV s^{-1}).

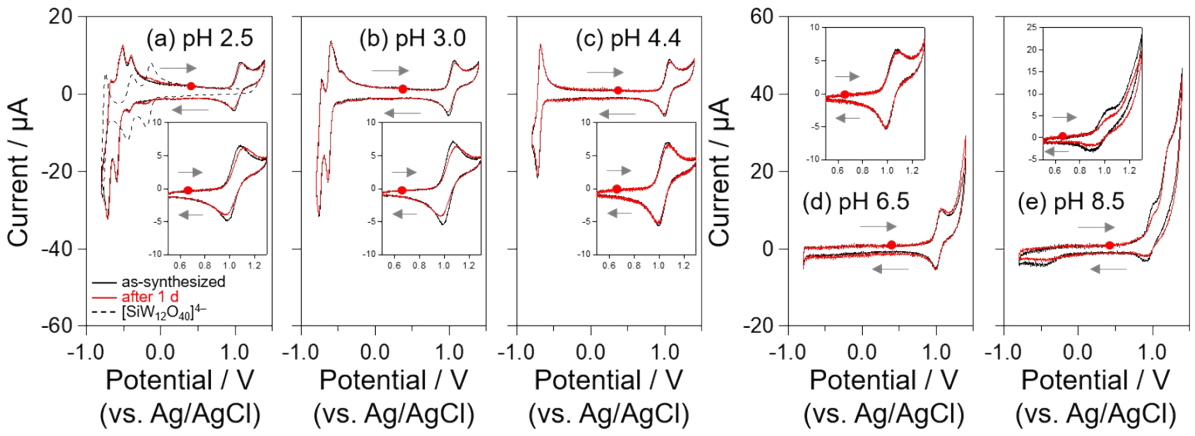

Fig. S3 Cyclic voltammograms of SiCo (1 mM) in aq. $K_xH_{3-x}PO_4$ solutions (0.5 M) at different pH conditions after 1 d (working electrode: GC, counter electrode: Pt coil; scan rate: 50 mV s^{-1}).

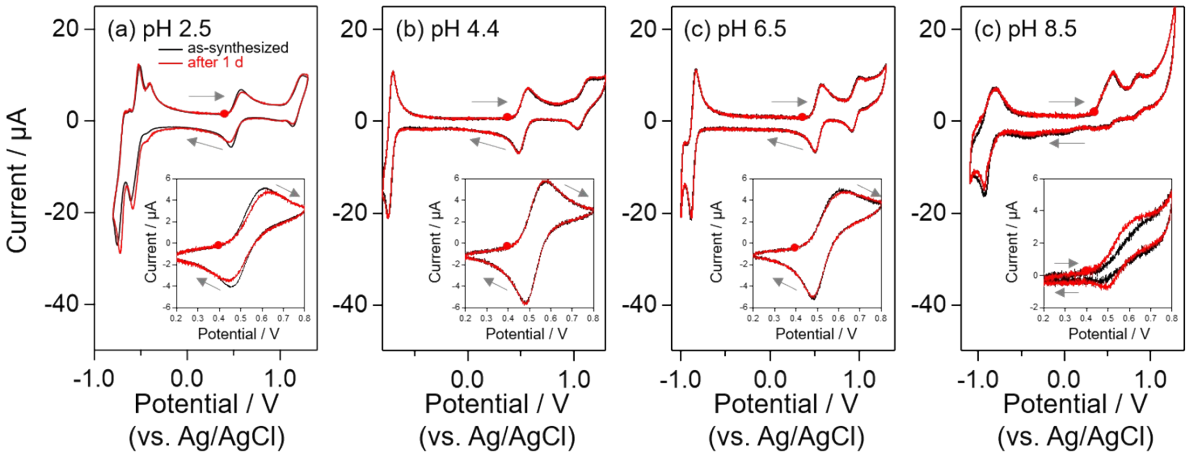

Fig. S4 Cyclic voltammograms of SiMn (1 mM) in aq. $K_xH_{3-x}PO_4$ solutions (0.5 M) at different pH conditions after 1 d (working electrode: GC, counter electrode: Pt coil; scan rate: 50 mV s^{-1}).

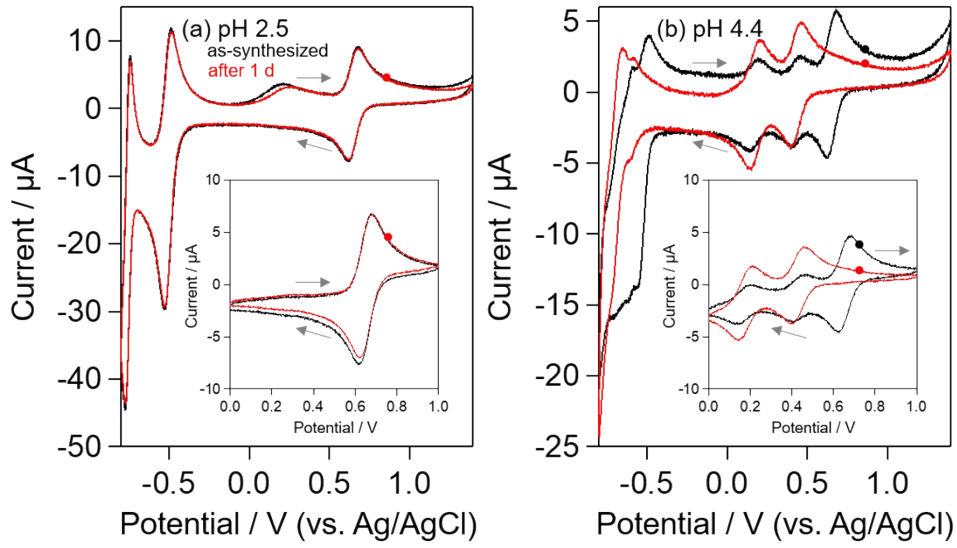

Fig. S5 Cyclic voltammograms of PV (1 mM) in aq. $K_xH_{3-x}PO_4$ solutions (0.5 M) at different pH conditions after 1 d (working electrode: GC, counter electrode: Pt coil; scan rate: 50 mV s^{-1}).

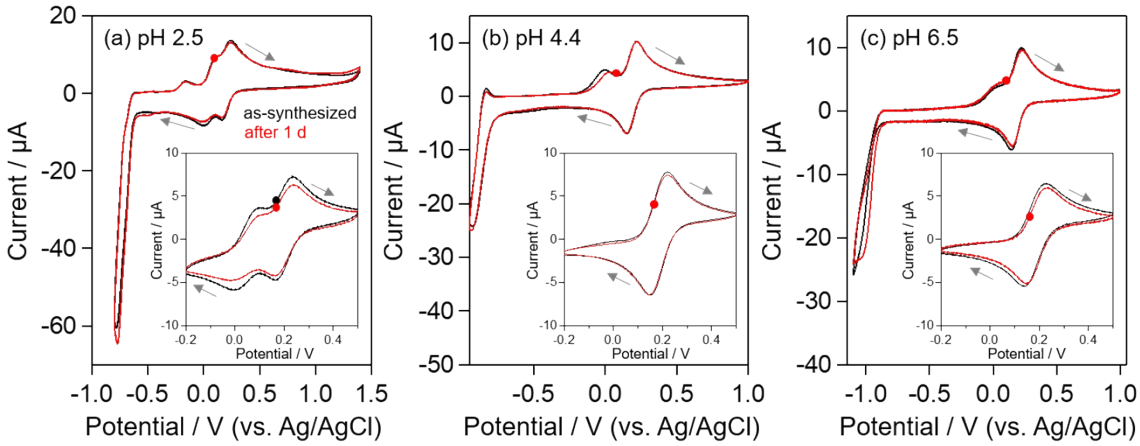

Fig. S6 Cyclic voltammograms of BV (1 mM) in aq. $K_xH_{3-x}PO_4$ solutions (0.05 M) at different pH conditions after 1 d (working electrode: GC, counter electrode: Pt coil; scan rate: 50 mV s^{-1}).

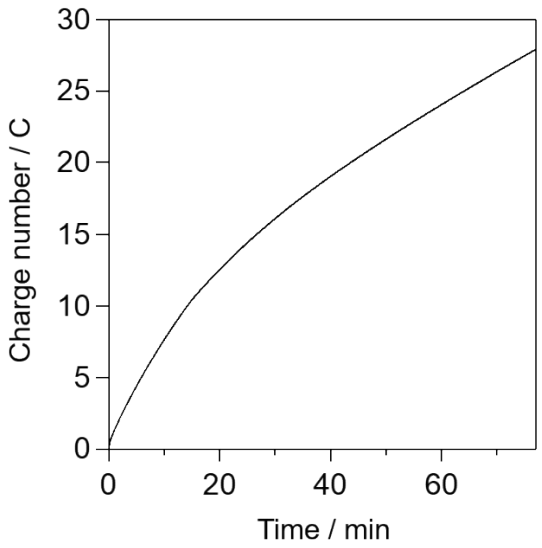

Fig. S7 Time courses of the charge number passing through the outer circuit during the electrochemical oxidation of $SiCo^{II}$ (1 mM) at +1.18 V (vs. Ag/AgCl) by controlled potential electrolysis in bulk electrolysis cell (supporting electrolyte: 0.5 M of aq. $K_xH_{3-x}PO_4$ solution (50 mL, pH 3.0)).

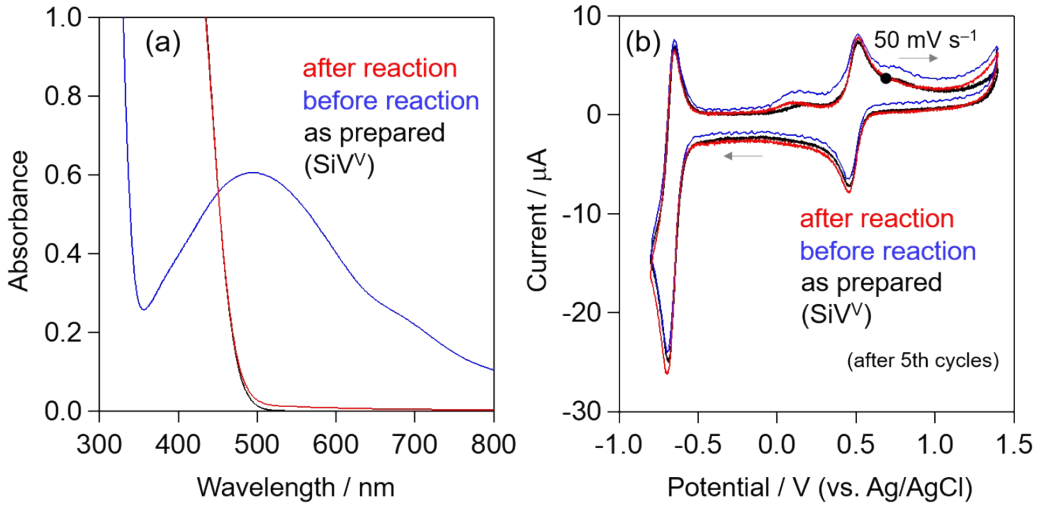

Fig. S8 (a) Absorption spectra and (b) cyclic voltammograms of solution containing SiV (1 mM) before and after photocatalytic H_2 evolution over $Ru/SrTiO_3$:Rh in aq. KH_2PO_4 solution (0.5 M, pH 4.4) (working electrode: GC, counter electrode: Pt coil; scan rate: 50 mV s^{-1}; initial scan direction: toward more positive potential).

Table S1 Initial rate of H_2 evolution over $Ru/SrTiO_3$:Rh photocatalyst particles suspended in aq. KH_2PO_4 solutions under visible light.

Electron donor	Concentration of reduced specie / mM	Concentration of oxidized specie / mM	Initial rate of H_2 evolved / μmol h^{-1}
SiV^{IV}	1	0	6.9
	0.5	0	5.3
	1	0.5	4.6
$SiMn^{II}$	1	0	8.0
	0.5	0	6.9
	1.0	0.5	6.2

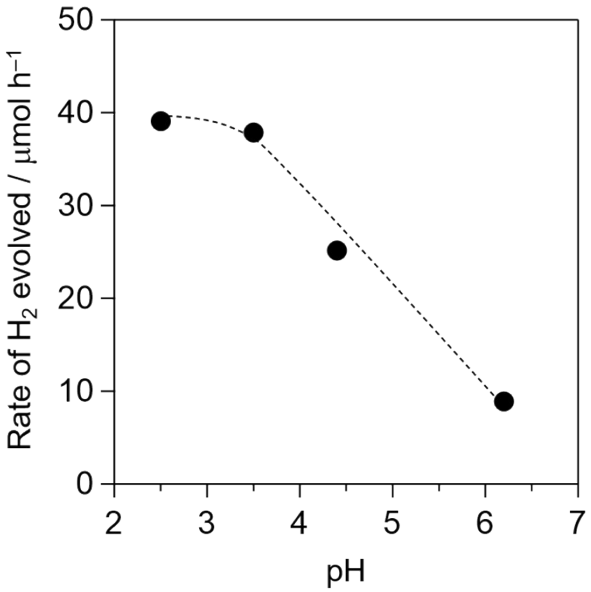

Fig. S9 Relation between the pH of reaction solution (adjusted with 0.1 M of H_2SO_4) and the rates of photocatalytic H_2 evolution from an aq. MeOH solution under visible light irradiation.

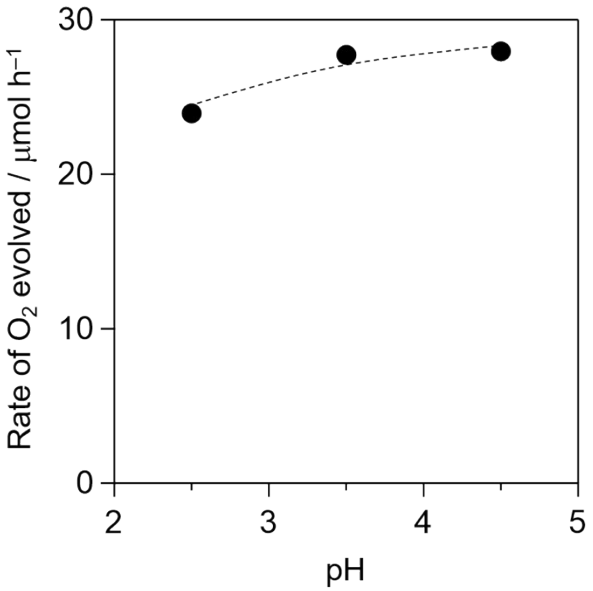

Fig. S10 Relation between the pH of reaction solution (adjusted with 0.1 M of HNO_3) and the rates of photocatalytic O_2 evolution from an aq. solution containing Ag^+ (10 mM, 100 mL) under visible light irradiation.

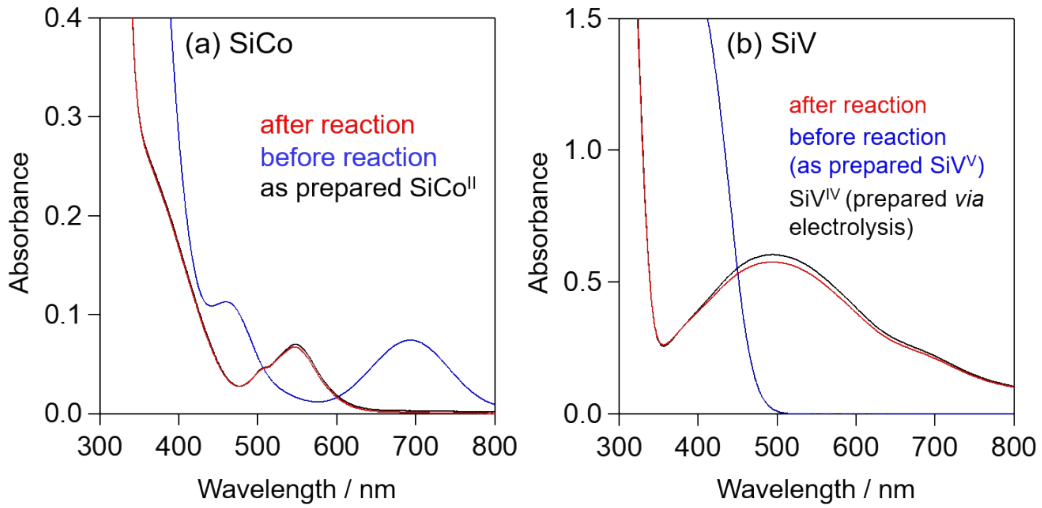

Fig. S11 Absorption spectra of aq. $K_xH_{3-x}PO_4$ solution (0.5 M) containing (a) SiCo (1 mM, pH 3.0) and (b) SiV (1 mM, pH 4.4) before and after photocatalytic O_2 evolution over PtO_x/WO_3.

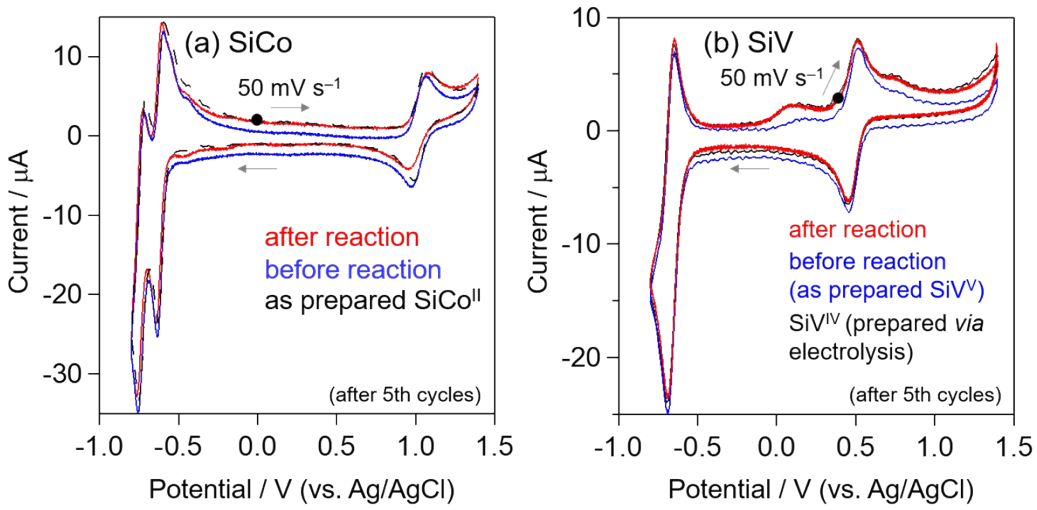

Fig. S12 Cyclic voltammograms of aq. KH_2PO_4 solution (0.5 M) containing (a) SiCo (1 mM, pH 3.0) and (b) SiV (1 mM, pH 4.4) before and after photocatalytic O_2 evolution over PtO_x/WO_3 (working electrode: GC, counter electrode: Pt coil; scan rate: 50 mV s^{-1}; initial scan direction: toward more positive potential).

Table S2 Initial rate of O_2 evolution over PtO_x/WO_3 photocatalyst particles suspended in aq. KH_2PO_4 solutions under visible light.

Electron acceptor	Concentration of oxidized specie / mM	Concentration of reduced specie / mM	Initial rate of O_2 evolved / μmol h^{-1}
SiV^V	1	0	2.4
	0.5	0	1.3
	1	0.5	0.4
$SiMn^{III}$	1	0	6.3
	0.5	0	3.5
	1.0	0.5	2.7

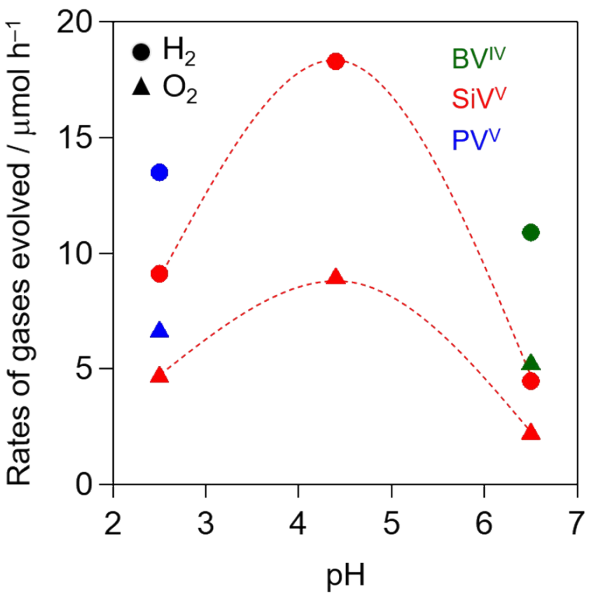

Fig. S13 Initial rates of gases evolved from aq. $K_xH_{3-x}PO_4$ solutions (0.05 M, 100 mL) over PtO_x/WO_3 (0.3 g) and Ru/$SrTiO_3$:Rh (0.1 g) containing XV^{IV} (X = Si, P, or B) (0.5 mM each) under visible light.

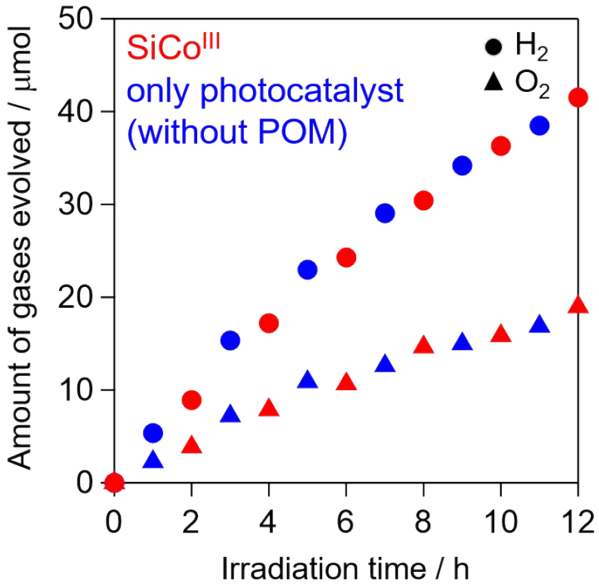

Fig. S14 Time courses of photocatalytic gases evolution using a mixture of PtO_x/WO_3 (0.3 g) and Ru/$SrTiO_3$:Rh (0.1 g) suspended in aq. KH_2PO_4 solution (0.05 M, 100 mL, pH 4.4) containing SiCo^{III} under visible light.

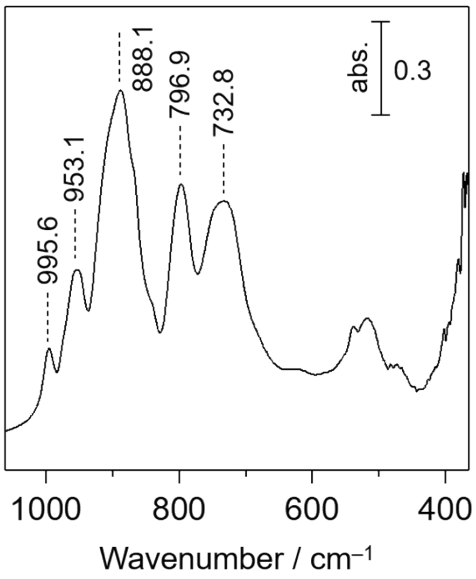

Fig. S15 FT-IR spectrum of lacunary polyoxometalate (SiW_{11}) (back ground: air; KBr: 1 wt.%).

Figs. S16-S19 shows the Negative ion ESI mass spectrum. Several peaks which were assignable to protonated and/or dehydrated form of desired polyoxoanions were observed.

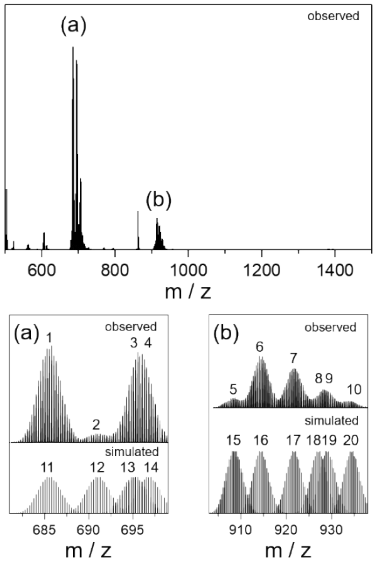

peak	m/z
1	685.31
2	690.29
3	695.54
4	696.80
5	908.07
6	914.07
7	921.40
8	928.06
9	929.38
10	933.71
11	685.30
12	690.79
13	695.29
14	696.54
15	908.40
16	914.07
17	921.39
18	927.39
19	928.72
20	934.71

Fig. S16 Negative ion ESI mass spectrum of SiV^{V} prepared, along with that of simulated mass peaks.

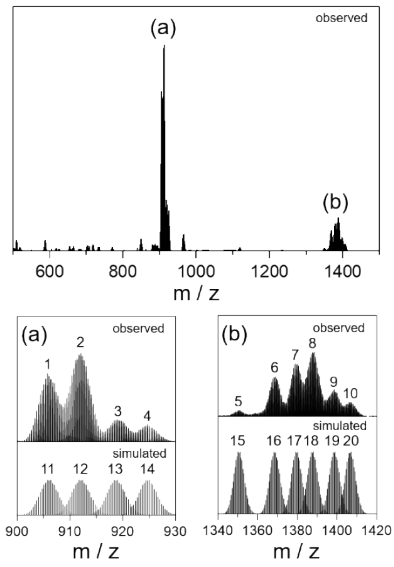

peak	m/z
1	905.06
2	912.41
3	919.06
4	925.05
5	1350.60
6	1368.12
7	1379.08
8	1387.57
9	1399.05
10	1407.06
11	905.73
12	911.73
13	919.05
14	925.05
15	1350.09
16	1368.10
17	1379.09
18	1388.08
19	1399.07
20	1407.06

Fig. S17 Negative ion ESI mass spectrum of $SiCo^{II}$ prepared, along with that of simulated mass peaks.

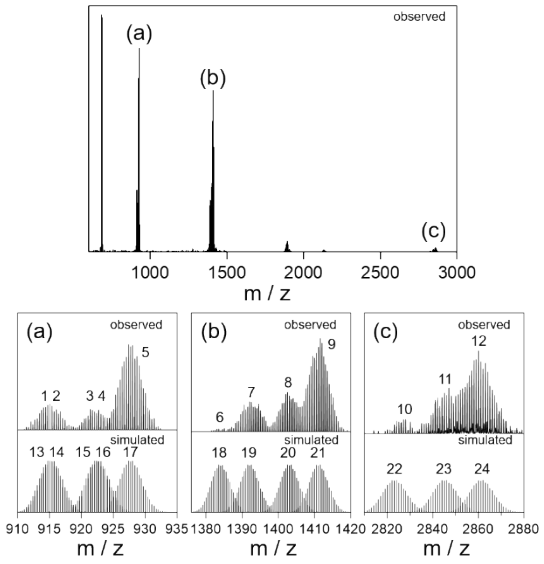

peak	m/z
1	914.73
2	915.06
3	922.06
4	922.39
5	927.38
6	1383.59
7	1392.07
8	1402.56
9	1411.55
10	2825.11
11	2846.09
12	2862.08
13	914.73
14	915.06
15	922.06
16	922.39
17	927.38
18	1383.59
19	1391.57
20	1402.56
21	1411.55
22	2824.11
23	2846.10
24	2862.07

Fig. S18 Negative ion ESI mass spectrum of PV^{V} prepared, along with that of simulated mass peaks.

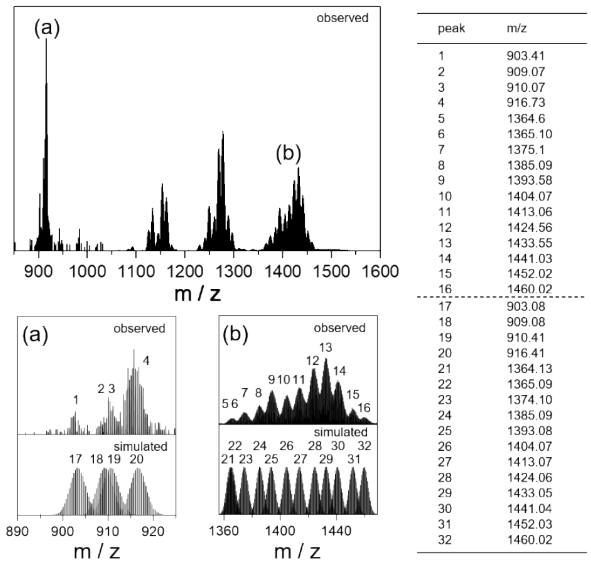

peak	m/z
1	903.41
2	909.07
3	910.07
4	916.73
5	1364.6
6	1365.10
7	1375.1
8	1385.09
9	1393.58
10	1404.07
11	1413.06
12	1424.56
13	1433.55
14	1441.03
15	1452.02
16	1460.02
17	903.08
18	909.08
19	910.41
20	916.41
21	1364.13
22	1365.09
23	1374.10
24	1385.09
25	1393.08
26	1404.07
27	1413.07
28	1424.06
29	1433.05
30	1441.04
31	1452.03
32	1460.02

Fig. S19 Negative ion ESI mass spectrum of BV^{IV} prepared, along with that of simulated mass peaks.

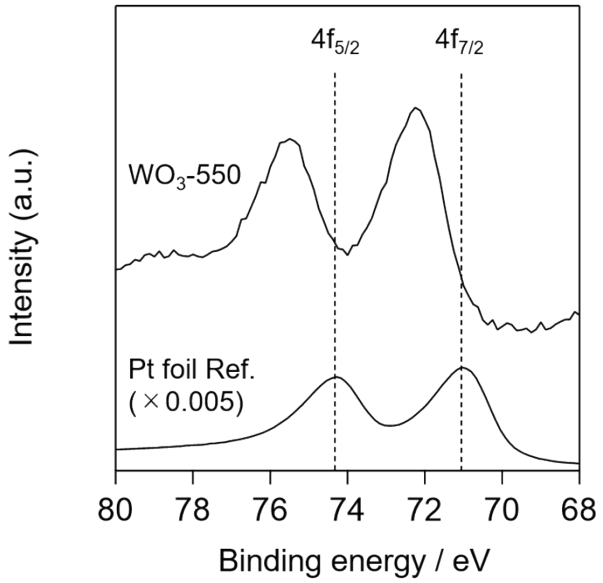

Fig. S20 XP spectra of WO_3 samples loaded with Pt species prepared *via* impregnation followed by the calcination in air (Amount of Pt : 0.5 wt.%), along with that of Pt foil for comparison.